

# Mineralogy And Geochemistry of Heavy Mineral Beach-Placer Sandstones in New Mexico

**Evan J. Owen**

NM Bureau of Geology and Mineral Resources,  
New Mexico Tech, Socorro, NM

**Virginia T. McLemore**

NM Bureau of Geology and Mineral Resources,  
New Mexico Tech, Socorro, NM

## ABSTRACT

Heavy mineral beach-placer sandstones are accumulations of high specific gravity, resistant minerals that form from mechanical concentration by waves, currents, and winds in marginal-marine environments. These sediments are enriched in critical minerals such as titanium, zirconium, and REE. Cretaceous beach-placer sandstones are found in the Colorado Plateau of northwestern New Mexico. Originally discovered by airborne radiometric surveys for uranium in the 1950s, these beach-placer sandstones are being re-examined with modern methods as potential sources for critical minerals. Selected beach-placer sandstones have been sampled, mapped with ground radiometric surveys, and analyzed with whole-rock and trace element geochemical methods. Mineralogy is being determined with optical methods, XRD, and EMPA. Zircon, rutile, ilmenite, and monazite are the primary heavy minerals of interest found in the studied deposits. Initial results show that the sandstones contain up to 1.4% total REE, 29.4% TiO<sub>2</sub>, and an estimated 4.9% ZrO<sub>2</sub>. Chondrite-normalized REE diagrams show distinct light REE and minor heavy REE enrichment, as well as pronounced negative Eu anomalies for each deposit.

## INTRODUCTION

Heavy mineral beach-placer sandstones are accumulations of high specific gravity, resistant minerals that form from mechanical concentration by waves, currents, and winds in marginal-marine environments (Van Gosen et al., 2014). These sandstones contain minerals such as zircon, rutile, ilmenite, and monazite, sources of critical minerals such as zirconium, titanium, and rare earth elements (REE). Critical minerals are mineral commodities that are essential to the economic and national security of the United States (Ellis, 2018). The United States is 100% import reliant on many critical minerals and are currently sourcing them from countries that can easily disrupt supply chains. These commodities are also required for modern electronics, as well as in technology for the green energy transition, such as wind turbines, solar panels, and electric cars (Goodenough, 2018).

Cretaceous heavy mineral sandstones are found in the Colorado Plateau within the San Juan Basin in northwestern New Mexico (Dow and Batty, 1961; McLemore, 2010; 2016; 2017). This Upper Cretaceous-Early Tertiary age structural basin extends into southern Colorado and contains significant coal, uranium, petroleum, and natural

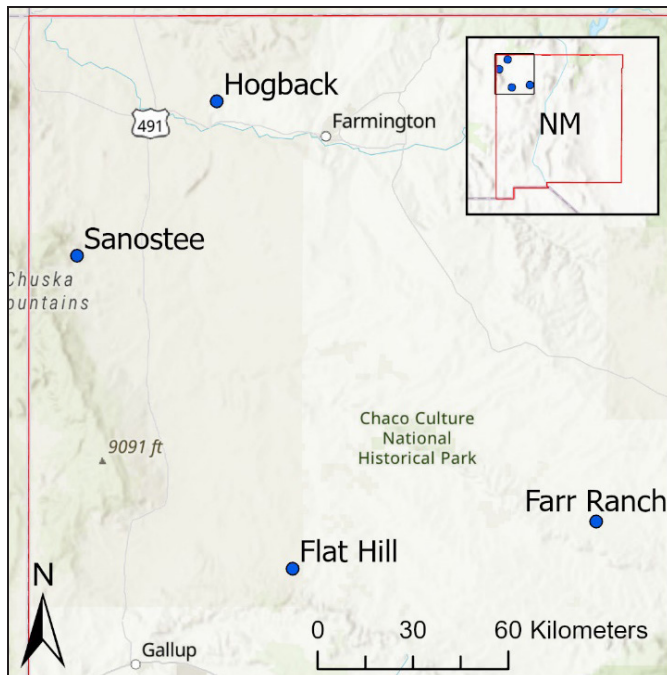


**Figure 1. Map of northwestern New Mexico showing the locations of the four heavy mineral sandstone deposits described in this study**

gas resources. Many of the heavy mineral sandstone deposits were discovered in the 1950s by airborne radiometric surveys for uranium, as the deposits are radioactive due to elevated uranium and thorium found within monazite and zircon, primarily. Previous studies by McLemore (2010, 2016, 2017) have examined numerous heavy mineral sandstones in the San Juan Basin of New Mexico, compiling historic data, as well as collecting new data including petrography and geochemical analyses. The New Mexico Bureau of Geology and Mineral Resources is currently reinvestigating heavy mineral sandstones in the state as part of the U.S. DOE CORE-CM (Carbon Ore, Rare Earth and Critical Minerals) Initiative. Several heavy mineral sandstone deposits have been recently sampled (Figure 1), mapped with ground radiometric surveys, and analyzed with whole-rock and trace element geochemical methods. Mineralogy and petrography currently source from previous studies, though new mineralogic and petrographic examinations will be presented in an upcoming report.

## METHODS

### Sample Collection

Select samples of variably mineralized sandstones were collected from each of the deposits. Color and density generally

correlate with mineralization, with dark, dense sandstones containing higher proportions of heavy minerals such as ilmenite, zircon, and monazite. A handheld scintillation counter (Exploranium GR-130) was used to identify and sample the most mineralized sandstones at each study site, though less mineralized to barren sandstones were also sampled. Hand samples and extra material for archive were collected alongside a split for geochemical analysis.

### Ground Radiometric Surveys

The handheld scintillation counter was also used in combination with a handheld GPS to create ground radiometric surveys over each study area. Survey grids were not planned ahead of time, but rather surveyed “on the fly,” with the edges of the survey extent generally defined by a return to background radiation values. This allowed the anomalies to more or less define themselves as they were surveyed. The scintillation counter was held at waist height and was allowed to equilibrate at each station. The reading at each station (in counts per second, cps) was recorded on a handheld GPS. Station spacing varied between site, but generally was ~15 m over mineralized zones up to 50 m over unmineralized areas. Radiometric maps were created using Esri ArcGIS Pro.

### Petrography and Mineralogy

Petrographic and mineralogic descriptions currently come from previous studies (McLemore, 2010; 2016; 2017; 2022) and those methods will be briefly summarized here. Polished thin sections were prepared and examined using standard petrographic microscopy, as well as scanning electron microscopy (SEM). Samples were also examined using a Cameca SX100 electron microprobe analyzer (EMPA) with three wavelength-dispersive spectrometers at the New Mexico Bureau of Geology and Mineral Resources. EMPA provided quantitative mineral chemistry of minerals of interest, as well as textural relationships using backscattered electron (BSE) imaging.

### Whole-rock and Trace Element Geochemistry

Existing whole-rock and trace element geochemistry was combined with new data generated from this project. ALS Global performed the geochemical analyses used in this study. The whole-rock and trace element geochemical methods used can be found at [www.alsglobal.com/en/geochemistry/geochemistry-fee-schedules](http://www.alsglobal.com/en/geochemistry/geochemistry-fee-schedules) and will be described in future reports. IMDEX ioGAS and Microsoft Excel were used to analyze and present geochemical data.

### Estimation of Combined Uranium and Thorium Content with a Scintillation Counter

Some samples exceeded the laboratory's upper detection limit for thorium (>1000 ppm Th). A simple method was developed to estimate total U and Th content in highly mineralized sandstones. Archive samples of 500g or more were weighed using a scale accurate to 0.5g. The Exploranium GR-130 handheld scintillation counter was placed on a stable surface away from other radioactive sources in order to have a low background radiation reading. The unit was run in the "survey" mode with 30 seconds between readings. The scintillation counter was allowed to equilibrate for at least one minute, and the background reading was recorded (counts per second, cps). Each sample was placed directly in front of the scintillation counter and was again allowed to equilibrate for at least one minute. Each sample's radioactivity was recorded. The background radiation reading was then subtracted from each sample's radioactivity. As the sample's radioactivity depends not only on its mass, but also its composition (U and Th content, K is not present in significant amounts), the sample's background subtracted radioactivity was divided by the sample's mass to create a "specific activity" for each sample. "Specific activity" is used here in quotes, as specific activity is defined as the activity per unit mass of a radionuclide in the field of nuclear physics. Here, "specific activity" refers to the activity per sample mass. By correlating these "specific activities" to known U+Th values, the resulting line of best fit can be used to estimate U+Th values from the easy to measure "specific activity" of unknown samples, provided they contain enough U and Th to measure above background radiation levels.

### RESULTS

Four sites containing heavy mineral sandstones have been recently studied for this project (Figure 1). The Hogback Deposit is located in San Juan County between Shiprock and Farmington. The Sanostee Deposit is located on the Navajo Nation in San Juan County south of Shiprock. The Flat Top Hill Deposit (also known as Standing Rock) is located in McKinley County on the Navajo Nation northwest of Crownpoint. The Farr Ranch Deposit (also known as Star Lake) is also located in McKinley County on the Navajo Nation and is southwest of Cuba.

#### Ground Radiometric Maps

Each area was surveyed with a handheld scintillation counter to help define the extent of the mineralized sandstones. Figures 2 through 5 show the results from these radiometric surveys.

The survey of the Sanostee Deposit (Figure 2) consisted of 234 stations focused around the ledges of the mesa where the most mineralized sandstones were exposed. The survey shows a 1200 meter long, northwest trending zone of mineralization that is likely shallowly buried under the thicker portion of the mesa and eroded away entirely between the central and northwestern portion of the deposit. The survey also shows a nearly 200 meter long, narrower mineralized zone southwest of the main zone of mineralization, also trending northwest. The most radioactive stations were above 2000 cps, with the highest value of 4500 cps located on the ledge at the very northwest extent of the survey. It is possible that these mineralized zones extend along strike to the northwest, but may be buried deeper. Extension to the southeast is also possible, but the mesa cliffs out around 600 meters from the southern end of the surveyed area.

The survey of the Flat Top Hill Deposit (Figure 3) consists of two separate mineralized zones that lie on strike with each other. Flat Top Hill, host to what is referred to here as Flat Top Hill East Deposit, is an 800 meter long, northwest oriented mesa with distinct incisions on its northeast face. The extension of this deposit, referred to as Flat Top Hill West, lies roughly 1.6 kilometers to the northwest on a less prominent, narrow ridge roughly 1.3 kilometers long. The radiometric survey of Flat Top Hill East consisted of

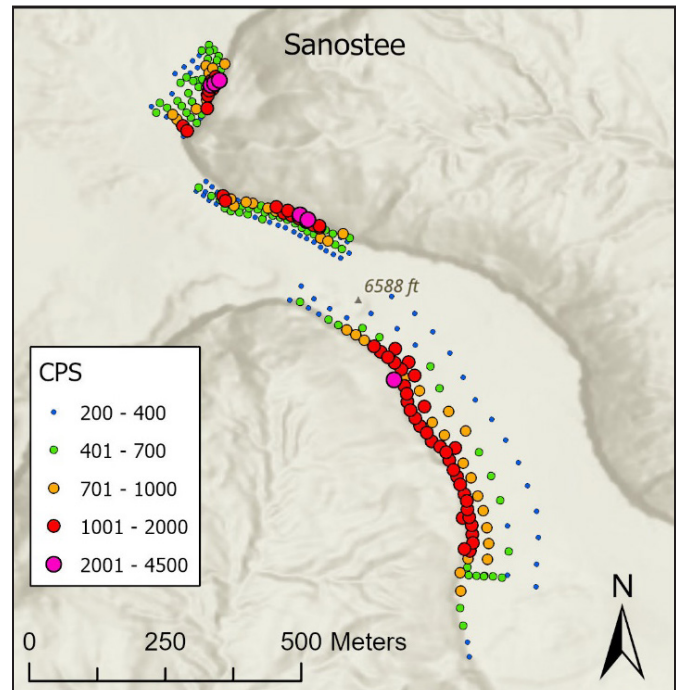
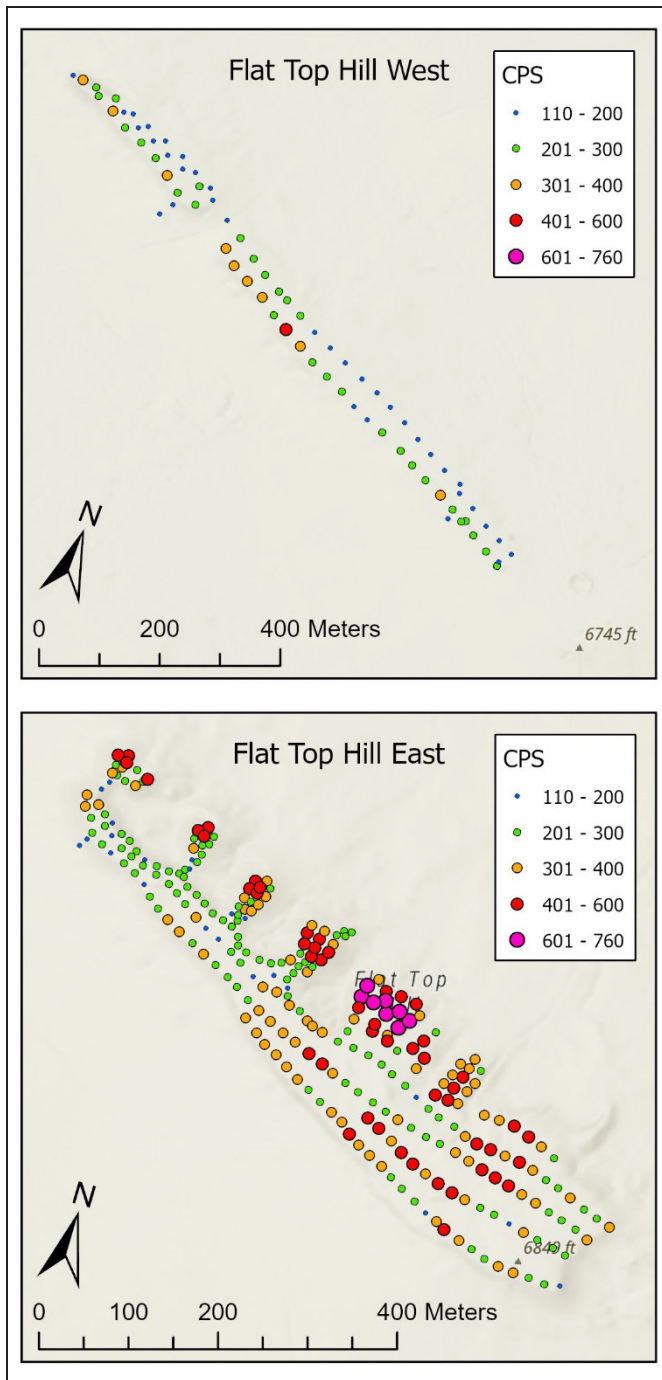


Figure 2. Ground radiometric survey of the Sanostee Deposit showing a 1200 meter long zone of mineralized heavy mineral sandstone and a less extensive zone to the southwest of the northern end



**Figure 3. Ground radiometric survey of the Flat Top Hill East and West Deposits. Flat Top Hill East shows the most mineralized zones along the “fingers” extending towards the northeast. Flat Top Hill West is less mineralized, with its most elevated values lying on the southeast edge of the ridge**

273 stations and shows that the most radioactive zones lie on the “fingers” that extend to the northeast. The highest values reach 760 cps. Elevated values are also found on the wider, southeastern portion of the mesa. As radioactivity

decreased in lower elevation portions of the mesa, it is likely that the mineralized horizon has been locally eroded. The survey of Flat Top Hill West was comprised of 75 stations. The most radioactive zones are generally confined to the southwestern edge of the ridge, with the highest value reaching 420 cps. This deposit appears to be less mineralized or more eroded (or both) than Flat Top Hill East. No other apparent northwest trending mesas or ridges appear in the vicinity of Flat Top Hill, so it is unlikely that these deposits continue elsewhere.

The Farr Ranch Deposit (Figure 4) lies on a 1.2 kilometer long, northwest trending, southwest sloping mesa with a steep northeast face. 71 stations were surveyed over this deposit. The zones of highest radioactivity were located on the northwest-central portion of the mesa and reached 1200 cps. Similar to Flat Top Hill, lower elevations on the mesa corresponded with lower radioactivity, suggesting erosion of the mineralized sandstone.

The Hogback Deposit is so named because it lies along the Hogback near Shiprock. The radiometric survey over the deposit (Figure 5) consists of 82 stations on a southeast sloping hill on the west side of Coal Mine Creek. Unlike the other surveyed deposits, the Hogback Deposit appears to exhibit less topographic control than the deposits found on relatively prominent mesas or ridges. The radiometric

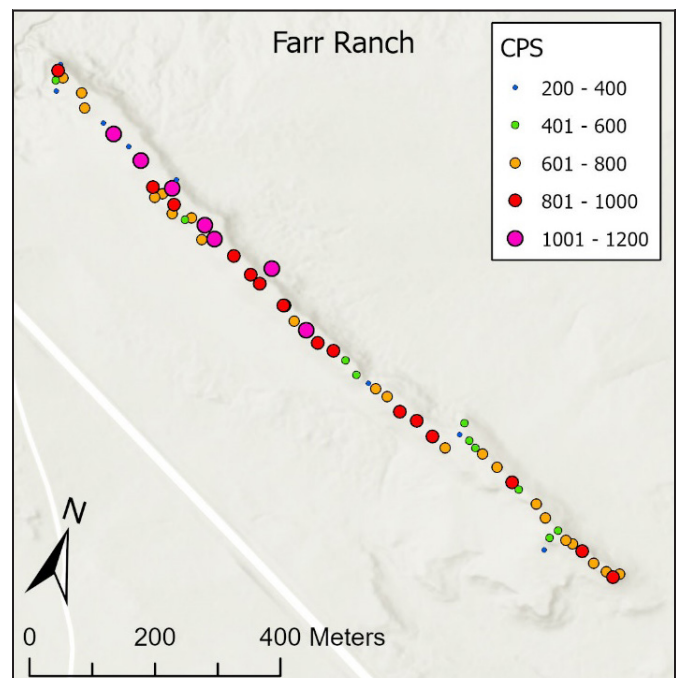


**Figure 4. Ground radiometric survey of the Farr Ranch Deposit showing a northwest trending mesa with zones of highest radioactivity located towards the northwest end of the mesa**

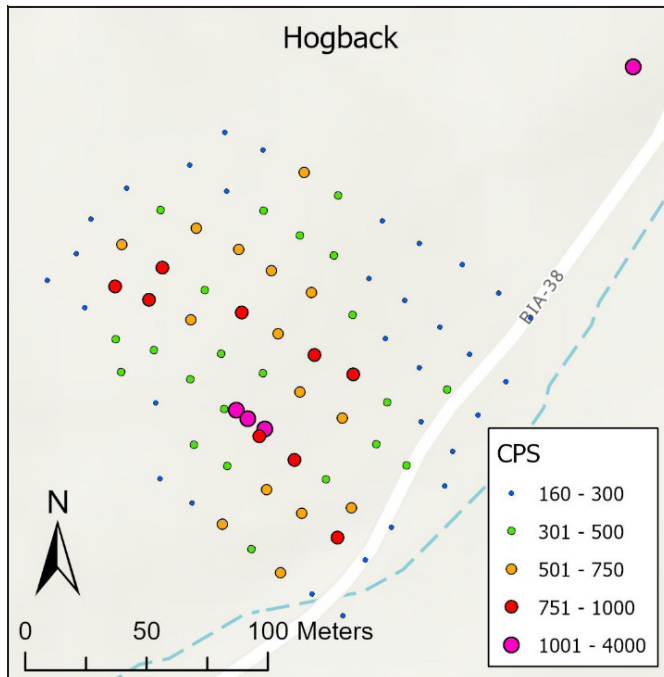


**Figure 5. Ground radiometric survey of the Hogback Deposit showing a north to northwest trending radiometric anomaly. A possible stockpile of mineralized sandstone lies to the northeast of the main survey area**

anomaly forms a north to northwest feature roughly 200 meters long. The most radioactive zone within the anomaly reaches 1500 cps. An even more radioactive zone was located 120 meters northeast of the main surveyed area and reached 4000 cps. This zone appeared to be a stockpile of mineralized sandstone from historic prospecting efforts.

### Petrography and Mineralogy

Petrographic and mineralogic descriptions of these heavy mineral sandstones will be briefly discussed here as they are critical to the potential economics of these deposits, however, more detailed petrography and mineral analysis is planned for a future report. In general, the mineralogy of the heavy mineral sandstones in New Mexico is simple, consisting primarily of variable amounts of ilmenite ( $\text{FeTiO}_3$ ), rutile ( $\text{TiO}_2$ ), zircon ( $\text{ZrSiO}_4$ ), monazite ( $[\text{Ce},\text{La}]\text{PO}_4$ ) with gangue quartz cemented by iron oxides. The sandstones are generally fine-grained and well sorted with subrounded to rounded clasts. Zircon crystals may still show terminations as a result of its high hardness. Figure 6 shows a BSE photomicrograph from a previous study (McLemore and Robison, 2016) of a characteristic heavy mineral sandstone from the Sanostee Deposit with grains of zircon, ilmenite, and monazite amongst subrounded quartz cemented by iron oxides. Future mineralogical studies will

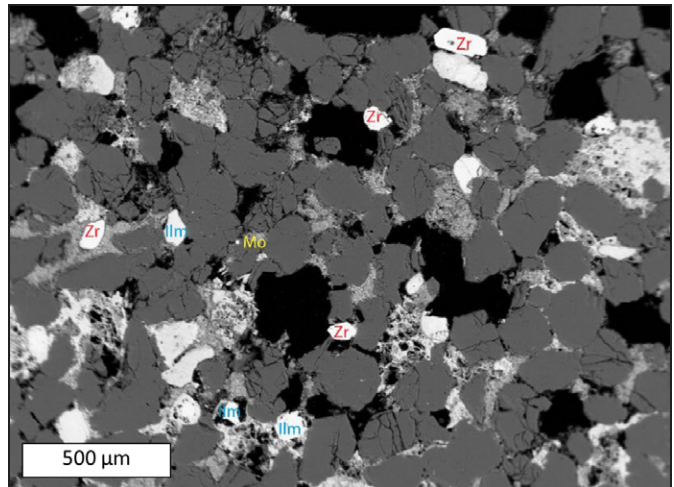


**Figure 6. BSE photomicrograph of a heavy mineral sandstone from the Sanostee Deposit. This sample shows zircon grains (some of which are euhedral), ilmenite, and monazite with subrounded quartz cemented by iron oxides. From McLemore and Robison (2016)**

examine the rare earth element distribution between zircon and monazite.

### Whole-Rock and Trace Element Geochemical Data

Newly generated whole-rock and trace element geochemical data has been combined with existing geochemical data from an investigation of the heavy mineral sandstone deposit at Apache Mesa on the Jicarilla Apache Reservation in Rio Arriba County (McLemore et al., 2016). 49 new samples were collected over the four surveyed sites described above. 44 geochemical samples exist from the Apache Mesa project. More recent data was favored over historic data in this study because of the lower detection limits for many analytes, as well as analyses for the entire suite of REE. Table 1 presents a summary of elements of interest from this dataset. Notably, some analytes reach very elevated values:  $\text{TiO}_2$  (29.4%), total REE + Y (1.4%), Zr (>1%), Th (>0.1%), Hf (0.16%).

Samples show distinct light REE enrichment and slight heavy REE enrichment compared to C1 chondrite values (Figure 7; McDonough and Sun, 1995) with prominent

**Table 1. Summary statistics of selected elements in heavy mineral sandstones**

| n=93           | $\text{SiO}_2$<br>(%) | $\text{Fe}_2\text{O}_3$<br>(%) | $\text{TiO}_2$<br>(%) | Hf<br>(ppm) | Th<br>(ppm) | U<br>(ppm) | Zr<br>(ppm) | TREE+Y<br>(ppm) |
|----------------|-----------------------|--------------------------------|-----------------------|-------------|-------------|------------|-------------|-----------------|
| <b>Minimum</b> | 4.67                  | 0.30                           | 0.08                  | 1.4         | 2.44        | 0.9        | 43          | 47              |
| <b>Maximum</b> | 96.13                 | 69.52                          | 29.4                  | 1630        | >1000       | 179.5      | >10000      | 14041           |
| <b>Mean</b>    | 58.99                 | 19.47                          | 5.42                  | 176.2       | 128.9       | 20.9       | 3913        | 1473            |
| <b>Median</b>  | 63.38                 | 12.77                          | 2.39                  | 38.9        | 31.6        | 7.8        | 1730        | 502             |

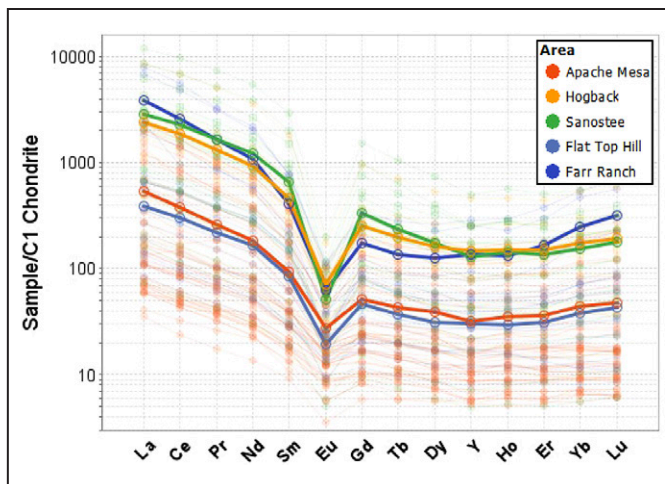


Figure 7. C1 chondrite-normalized spider diagram (McDonough and Sun, 1995) of heavy mineral sandstones showing highly elevated REE, distinct light REE enrichment, slight heavy REE enrichment, and prominent negative Eu anomalies

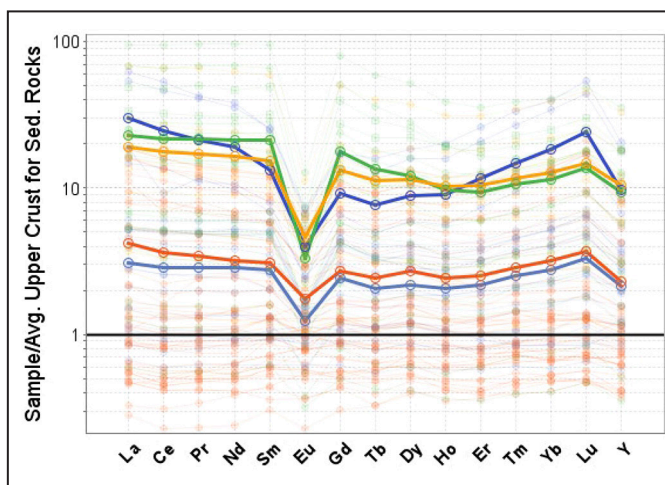


Figure 8. Average Upper Crust for Sedimentary Rocks-normalized spider diagram (Taylor and McLennan, 1981) of heavy mineral sandstones showing highly elevated REE,, slight heavy REE enrichment, and prominent negative Eu anomalies. Legend in Figure 7

negative Eu anomalies. This pattern may be explained by the combination of the light REE content of monazite combined with a preference for heavy REE substitution in zircon.

These heavy mineral sandstone samples were also normalized to the Average Upper Crust for Sedimentary Rocks standard (Figure 8; Taylor and McLennan, 1981). This plot shows overall enrichment of REE with prominent negative Eu anomalies and slight heavy REE enrichment, especially for Farr Ranch samples.

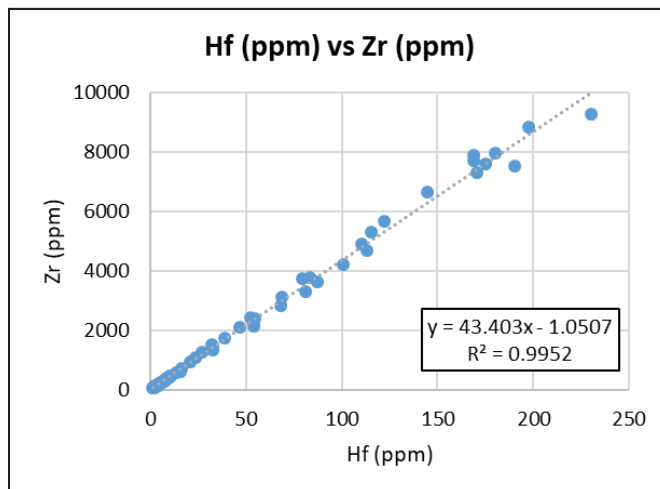
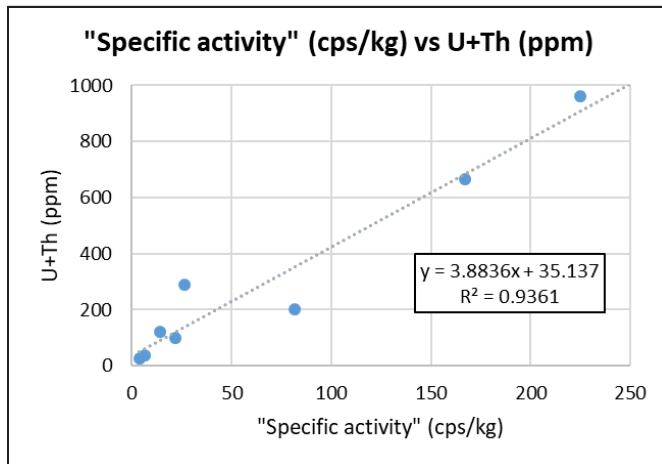


Figure 9. XY plot of Hf versus Zr showing an extremely strong positive correlation

Table 2. Laboratory data and extrapolations of Zr from Hf and total REE and U+Th from “specific activity.” Values in bold correspond with laboratory values above detection limits

| Sample | Laboratory data      |          |              |            | Extrapolations   |                         |                         | "Specific activity" (cps/kg) |
|--------|----------------------|----------|--------------|------------|------------------|-------------------------|-------------------------|------------------------------|
|        | TiO <sub>2</sub> (%) | Zr (ppm) | TREE+Y (ppm) | U+Th (ppm) | Zr (ppm) from Hf | TREE (ppm) from Sp.act. | U+Th (ppm) from Sp.act. |                              |
| Flat12 | 8.74                 | 7280     | 810          | 120.5      | 7399             | 1623                    | 89                      | 13.8                         |
| Flat13 | 2.34                 | 1060     | 321          | 27.3       | 1041             | 1430                    | 50                      | 3.8                          |
| Flat18 | 0.58                 | 204      | 150          | 7.9        | 193              |                         |                         | nd                           |
| Hog10  | 6.89                 | 3780     | 1446         | 99.0       | 3627             | 1773                    | 119                     | 21.6                         |
| Hog16  | 6.08                 | 8830     | 1951         | 202.9      | 8571             | 2932                    | 352                     | 81.6                         |
| Hog17  | 23.60                | >10000   | 9908         | >1000      | <b>49044</b>     | 5360                    | <b>840</b>              | 207.3                        |
| SAN 6  | 16.90                | >10000   | 9628         | >1000      | <b>17230</b>     | 11872                   | <b>2149</b>             | 544.4                        |
| SAN54  | 0.23                 | 264      | 86           | 8.3        | 295              |                         |                         | nd                           |
| SAN56  | 1.10                 | 1340     | 255          | 35.5       | 1431             | 1476                    | 59                      | 6.2                          |
| SAN57  | 18.55                | >10000   | 4981         | 664.6      | <b>32334</b>     | 4581                    | 684                     | 167.0                        |
| SAN58  | 8.21                 | 9280     | 2222         | 289.8      | 9982             | 1868                    | 138                     | 26.5                         |
| SAN60  | 16.55                | >10000   | 7093         | 959.9      | <b>28167</b>     | 5700                    | 909                     | 224.9                        |

The upper limit of detection for Zr in the trace element geochemical analysis package ordered from ALS Global is 10,000 ppm. Many of the highly mineralized heavy mineral sandstones broke this threshold. Rather than reorder an analysis for this overage, a simple method was developed to estimate the Zr concentration of highly mineralized sandstones. Hf is found nearly solely within zircon as a minor substituting element. Figure 9 shows that Hf and Zr correlate extremely positively (R<sup>2</sup>=0.9952) for samples of known Zr concentration (<10,000 ppm Zr). Thus, Hf can be used to extrapolate Zr values for samples that contain over 1% Zr by using the equation of the line of best fit shown in Figure 9. The results from this extrapolation are shown in Table 2, notably showing that one sample contains nearly 5% Zr.



**Figure 10. XY plot of “specific activity” versus combined U and Th showing a very strong positive correlation**

### Estimation of Combined Uranium and Thorium Content with a Scintillation Counter

Using the method described in the methods section, U+Th content can be estimated using a handheld scintillation counter. The “specific activity” of a subset of samples (n=12) with known U and Th concentrations from three deposits were correlated with their combined U and Th content (Figure 10). The resulting plot shows a very strong positive correlation ( $R^2=0.9361$ ), demonstrating that this method may be reasonable for estimating the combined U and Th content of unknown samples. Like the estimation of Zr from Hf, the equation from the line of best fit is used to extrapolate combined U and Th content from “specific activity.” The method has a sensitivity of around 30 ppm U+Th with the setup used here, though this could likely be improved upon by shielding the scintillation counter with lead to reduce the background radiation. The results from this experiment are shown in Table 2 and estimate that one sample contains over 2000 ppm U+Th. This method was also tested to see if it could reasonably estimate the total REE content of mineralized samples. Of the 12 samples investigated, this method overestimated two samples (FLAT13 and SAN56) by over five times the lab-determined total REE content and underestimated one sample (Hog17) by nearly 50%. While not as reliable as estimations of U+Th, this method may still have merit, especially if developed from samples from only one deposit, where the proportions of heavy minerals may be more consistent.

### PRELIMINARY CONCLUSIONS

New Mexico’s heavy mineral sandstone deposits are worth reinvestigating for their critical mineral potential, as the

economics of these commodities may change in the future. The use of handheld scintillation counters greatly aids in determining the extent of mineralized sandstones, as well as selecting high grade samples, due to the U and Th content of monazite and zircon, minerals found in relative abundance in these deposits. Whole-rock and trace element geochemical data show expectedly high values of critical minerals such as  $TiO_2$  (29.4%), total REE + Y (1.4%), Zr (>1%), and Hf (0.16%). C1 Chondrite-normalized diagrams show distinct light REE enrichment, slight heavy REE enrichment, and prominent negative Eu anomalies. Normalizing these samples to the Average Upper Crust for Sedimentary Rocks standard shows slight heavy REE enrichment and strong negative Eu anomalies. Hf can be used to accurately estimate Zr content for samples that pass the upper limit of detection of most trace element analysis suites (10,000 ppm Zr). Combined U and Th content can also be accurately estimated in mineralized sandstones by using a handheld scintillation counter to determine “specific activity,” subtracting the background radiation value from a sample’s radioactivity and dividing by its mass. The estimation of total REE using “specific activity” is less accurate, but might find use when working with samples from a single deposit. Future work will involve sampling other heavy mineral sandstone deposits in New Mexico and investigating the mineral chemistry of monazite and zircon in mineralized sandstones.

### ACKNOWLEDGMENTS

This report is part of on-going studies of mineral resources in New Mexico, supported by the New Mexico Bureau of Geology and Mineral Resources (NMBGMR), Nelia Dunbar, Director and State Geologist. Current research is funded through a DOE grant, Carbon Ore, Rare Earth, and Critical Minerals (CORE-CM) Assessment of San Juan River-Raton Coal Basin, New Mexico, DE-FE0032051. Any persons wishing to conduct geologic investigations on the Navajo Nation must first apply for and receive a permit from the Minerals Department, P.O. Box 1910, Window Rock, Arizona 86515, phone (928) 871-6588. Thanks to students of the NMBGMR Economic Geology group for assisting with sample handling.

### REFERENCES

- [1] Dow, V.T., & Batty, J.V., 1961, Reconnaissance of Titaniferous Sandstone Deposits of Utah, Wyoming, New Mexico, and Colorado. US Department of the Interior, Bureau of Mines.

- [2] Ellis, L., 2018, US Department of the Interior - Office of the Secretary: Final List of Critical Minerals 2018. Fed. Regist. 83, 23295–23296. Available at: [www.govinfo.gov/content/pkg/FR-2018-05-18/pdf/2018-10667.pdf](http://www.govinfo.gov/content/pkg/FR-2018-05-18/pdf/2018-10667.pdf).
- [3] Goodenough, K.M., Wall, F., and Merriman, D., 2018, The Rare Earth Elements: Demand, Global Resources, and Challenges for Resourcing Future Generations. Nat. Resour. Res. 27, 201–216.
- [4] Taylor, S.R., McLennan, S.M., Armstrong, R.L., & Tarney, J., 1981, The Composition and Evolution of the Continental Crust: Rare Earth Element Evidence from Sedimentary Rocks [and Discussion]. Philosophical Transactions of the Royal Society of London. Series A, Mathematical and Physical Sciences, 301(1461), 381–399. [www.jstor.org/stable/37026](http://www.jstor.org/stable/37026).
- [5] McDonough, W.F. and Sun, S.-s., 1995, The composition of the Earth. Chem. Geo. 120, 223–253.
- [6] McLemore, V.T., 2010, Distribution, origin, and mineral resource potential of Late Cretaceous heavy mineral, beach-placer sandstone deposits, in: Geology of the Four Corners Country, Fassett, James E.; Zeigler, Kate E.; Lueth, Virgil W., New Mexico Geological Society, Guidebook 61st Field Conference, pp. 197–212. [doi.org/10.56577/FFC-61.197](https://doi.org/10.56577/FFC-61.197).
- [7] McLemore, V.T., Asafo-Akowitz, J. and Robison, A., 2016, Assessment of Rare Earth Elements at Apache Mesa (Stinking Lake), Jicarilla Apache Reservation, Rio Arriba County, New Mexico: Final report to Jicarilla Indian Tribe, NMBG Open-file report 587, [geoinfo.nmt.edu/publications/openfile/details.cfm?Volume=587](http://geoinfo.nmt.edu/publications/openfile/details.cfm?Volume=587).
- [8] McLemore, V.T., & Robison, A., 2016, Exploration of Beach-Placer Heavy Mineral Deposits in the San Juan Basin in New Mexico: Society for Mining, Metallurgy, and Exploration. In 2016 Annual meeting Preprint (pp. 16–136).
- [9] McLemore, V.T., 2017, Heavy mineral, beach-placer sandstone deposits at Apache Mesa, Jicarilla Apache Reservation, Rio Arriba County, New Mexico; *in* The Geology of the Ouray-Silverton Area, Karlstrom, K.E., Gonzales, D.A., Zimmerer, M.J., Heizler, M., and Ulmer-Scholle, D.S.: New Mexico Geological Society 68th Annual Fall Field Conference Guidebook, p. 123–132.
- [10] Van Gosen, B.S., Fey, D.L., Shah, A.K., Verplanck, P.L., and Hoefen, T.M., 2014, Deposit model for heavy-mineral sands in coastal environments: U.S. Geological Survey Scientific Investigations Report 2010-5070-L, 51 p., [dx.doi.org/10.3133/sir20105070L](https://dx.doi.org/10.3133/sir20105070L).

# Minimizing Leaching of Al, Co, Cu, Fe, Li, and Ni During Discharge of Lithium-Ion Batteries

L. A. Sanchez-Calderon

Missouri Univ. of Science and Tech., Rolla, MO

L. Alagha

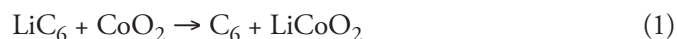
Missouri Univ. of Science and Tech., Rolla, MO

## ABSTRACT

The existing methods for recycling lithium-ion batteries present initial hurdles related to the safe handling and preparation of the batteries to avert potential explosions. Submerging batteries in sodium chloride (NaCl) solution has become an acceptable industrial practice. However, the use of NaCl to discharge lithium-ion batteries rusts the batteries' cases and releases metals which impacts the downstream processes that involve selective recovery of Li. This study aimed to determine the optimal concentrations and pH range of NaCl for the discharge of lithium-ion batteries for the purpose of minimizing the leach of Al, Co, Cu, Fe, Li, and Ni.

## INTRODUCTION

Lithium-ion batteries contain valuable metals like cobalt, copper, lithium, and nickel making its recycling economically very attractive (Ojanen et al., 2018). Recycling these metals also helps mitigate social and environmental impacts associated with mining practices of cobalt and lithium (Banza et al., 2009; Liu & Agusdinata, 2020). There are two main practices currently adopted by industry to recycle lithium-ion batteries. The first is the pyrometallurgy approach which consumes high energy and requires a high initial investment (Zhou et al., 2021). The second is the hydrometallurgical processing which requires discharging prior to leaching to avoid potential explosions (Liang et al., 2021). The discharge reaction is shown in Equation 1 (Bartholome et al., n.d.):



Lithium oxide is still reactive with water, but the reaction occurs at a slower rate than lithium metal with water.

There are primarily two methods for discharging a Li battery. The first involves connecting the battery to an electric circuit, which preserves the battery's shape and other conditions but is not practical for industrial-scale operations. The second method entails immersing the battery in an aqueous solution containing an electrolyte, typically NaCl. In the latter scenario, the NaCl solution serves as a conductive medium by facilitating the flow of electrons. The primary concern with the discharge processes with NaCl, or other media, is the corrosion of the battery casing and the release of metals. (Bae & Kim, 2021). The release of metals is undesirable as they can react with water, generating heat in the process. Moreover, the loss of valuable metals during the discharge process is economically unfavorable. Ultimately, it results in increased costs associated with treating the waste solutions to minimize environmental impacts. (Li et al., 2010).

To control the release of metals (i.e., Al, Co, Cu, Fe, Li, and Ni), this study proposed a 2-step procedure. The first step involved varying the concentration of NaCl in the submerging solution and studying its impact on battery case's corrosion rate at neutral pH. This aimed to select the optimal concentration at which the corrosion is minimal. In the second step, adjustments were made to the other key parameter, namely, pH. The pH is a critical factor as indicated by the Pourbaix diagram shown in Figure 1 (Barnes, 2014). The real challenge associated with this approach was to attain the maximum time limit of 16 hours, designed to ensure practicality in an industrial setting.